J.Serb.Chem.Soc. 68(11)893–901(2003)
JSCS – 3110

UDC 669.783+678.8+66.046.51:669.71.018
Original scientific paper

The effects of microalloying with silicon and germanium on microstructure and hardness of a commercial aluminum alloy

VESNA MAKSIMOVIĆ[1#], SLAVICA ZEC[1#], VELIMIR RADMILOVIĆ[2] and MILAN T. JOVANOVIĆ[1#]

[1]*Department of Materials Science, Vinča Institute of Nuclear Sciences, 11001 Belgrade, Serbia and Montenegro and* [2]*Department of Materials Science and Engineering, University of California, Berkeley, U.S.A.*

(Received 1 April, revised 26 June 2003)

Abstract: The effect of small additions of Si and Ge on the microstructure and hardness was investigated during aging of a commercial 2219 aluminum alloy. It was found that for the same level of microalloying in alloy 2219SG (containing Si and Ge), a maximum hardness was achieved 3 times faster than in alloy 2219S (without Ge). The accelerated precipitation kinetics is a consequence of the presence of fine Si–Ge particles, serving as heterogeneous precipitation sites for θ" strengthening particles.

Keywords: Al–Cu–Si–Ge alloys, Al alloy 2219, Si–Ge precipitate, heterogeneous precipitation, precipitate strengthening.

INTRODUCTION

There are several parameters which control the structure and properties of Al–Cu based alloys during the process of aging, such as: type (coherent or non-coherent), size, distribution and volume fraction of strengthening phase particles in the Al-based matrix. To promote a dense and homogeneous distribution of fine coherent precipitates, small amounts of Si, Mn, Be, Sn, Ag and Cd were added to an Al–Cu alloy.[1–5] Results of Hornbogen and co-workers[6,7] clearly demonstrated that in Al–Si–Ge alloys much finer Si–Ge precipitates (almost an order of a magnitude) may be achieved than in Al–Si and Al–Ge binary alloys. Very recently, Mitlin *et al.*[8–11] tried to modify the reaction of precipitation in Al–Cu alloy by the simultaneous addition of small amounts of Si and Ge (in total of 1 to 2 at.%) with the idea to control the kinetics of aging. Significant effects of strengthening have been achieved by this process through precipitation of θ' phase on finely dispersed Si and Ge particles. Due to the low concentration of Si and Ge additions, this concept of alloying may be regarded as microalloying.

Serbian Chemical Society active member.

It should be mentioned that the effect of Si and Ge on the reaction of precipitation was studied using an experimental quarternary Al–Cu–Si–Ge alloy.[8–11] However, elements such as Zr, V, Ti, Mn and Fe are always present in commercial aluminum alloys in order to control the grain size and to increase the temperature of recrystallization.[12] The effect of these elements on the chemical composition of the present phases and alloy properties must not be neglected.

The aim of this paper is to study the effect of small additions of Si and Ge on: (a) the microstructure and hardness, and (b) kinetics of precipitation of alloys based on a commercial 2219 aluminum alloy.

EXPERIMENTAL

A commercial 2219 aluminum alloy (fully corresponding to ASTM standard), produced by Kaiser Aluminum, was used as a starting material. In the next step the chemical composition of this alloy was modified since the total concentration of Si and Ge was anticipated to be about 0.5 at.%, with the Si/Ge ≈ 1 relation. Two experimental alloys were produced by this microalloying process, *i.e.,* one alloy (designated as 2219S) with higher concentration of Si than the standard ASTM alloy and another alloy with additions of both Si and Ge (designated as 2219SG). Spectrophotometry was used to determine the chemical composition of these alloys, which is shown in Table I. Concentration of most important elements is emphasized by framing.

TABLE I. The chemical composition of investigated alloys (mass %)

Element	2219 ASTM	2219 [at.%]	2219SC [at.%]
Cu	5.8–6.8	5.91 [2.52]	5.90 [2.52]
Ge	–	–	0.69 [0.26]
Si	max 0.2	0.51 [0.49]	0.28 [0.27]
Fe	max 0.3	0.24	0.26
Mn	0.2–0.4	0.28	0.29
Mg	max 0.02	0.01	0.01
Zn	max 0.1	0.05	0.06
Ti	0.02–0.1	0.08	0.08
Zr	0.1–0.25	0.12	0.13
V	0.05–0.15	0.09	0.09
Cr	–	0.007	0.007

Melting, microalloying with "master-alloys" (Al-12 mass % Si and Al-50 mass % Ge) and casting were performed in a one-chamber vacuum induction furnace "Degussa". Pouring was done in a graphite crucible.

After machining, ingots of 1 kg in weight each, were homogenized for 48 h at 500 ºC and hot-rolled from the starting thickness of 27 mm to a thickness of 2 mm. After hot-rolling, the heat treatment of samples was as follows:

a) annealing at 500 ºC for 24 h

b) water-quenching

c) holding at room temperature for 9 days (natural aging)

d) artificial aging at 190 ºC in the interval from 10 min to 300 h.

Rockwell macrohardness was measured using the B scale (1/16" diametar of ball, 100 kg load). Microstructural characterization was performed by the light microscope "Ziess Axiovert 25", scanning electron microscope (SEM) "JEOL JSM-5300" equipped with energy dispersive spectroscope (EDS), X-ray dif-

fraction equipment "Siemens D500" and transmission electron microscope (TEM) "JEOL 200 CX" operated at 200 kV. For light microscopy and SEM, samples were etched in a Keller solution consisting of 2 ml HF (48 %), 3 ml HCl (conc.), 5 ml HNO_3 (conc.) and 190 ml H_2O. Samples for TEM were thinned to electron transparency using a "Fischione" twin-jet apparatus. The electrolyte was 25 % solution of nitric acid in methanol and the thinning was carried out at –25 ºC at a voltage of 13 V that yielded a current of 50 mA. Only two sets of samples were studied by TEM: (a) aged for shorter times (corresponding to the maximum of hardness), and (b) aged for longer times (150 h).

RESULTS AND DISCUSSION

Microstructural investigation

Light microscopy. The microstructure of quenched samples is shown in Fig. 1 a,b.It is obvious that quenching did not produce a homogeneous microstructure which normally corresponds to the supersaturated solid solution. The presence of several phases of different morphology may be seen in the matrix of both alloys. The most prominent phase which appears in both alloys is in the form of light, plate-like particles with rounded edges, being larger in alloy 2219SG (about 20 μm in size). In addition, rod-like particles formed in parallel rows can be seen in the microstructure of 2219SG alloy (Fig. 1b).

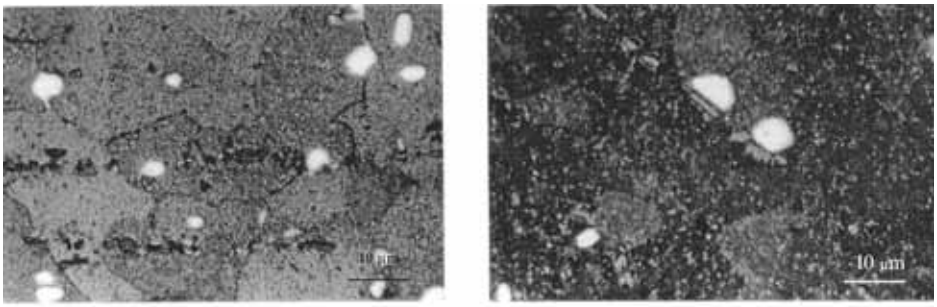

Fig. 1. Light microscopy. Microstructure of quenched samples. (a) Alloy 2219S; (b) alloy 2219SG.

SEM and EDS analysis. Microstructural details after quenching are shown in Fig. 2a,b, whereas results of EDS analysis of denoted particles are given in Table II. Results of Table II show that the thin and long particle (denoted as A) in alloy 2219S (Fig. 2a) consists of several elements, and it is likely that the chemical composition is similar to the phase of the type (Fe, Mn, Cu)$_3Si_2Al_{15}$ which appears in complex Al alloys.[13] On the other side, the chemical analysis of plate-like particle (B) in alloy 2219SG (Fig. 2b) suggests that it has a chemical composition close to that of a Al_7Cu_2Fe phase. The chemical composition of globular particles (C), appearing in both alloys, corresponds to the equilibrium Al_2Cu phase.

X-Ray diffraction. X-Ray diffraction patterns of quenched samples of both alloys are shown in Fig. 3a,b. In alloy 2219S (Fig. 3a), the existence of two phases was found, *i.e.*, an Al-based solid solution and the equilibrium θ phase (Al_2Cu). Apart from these two phases, peaks corresponding to a tetragonal lattice with parameters a = 0.6336 nm and c = 1.487 nm, were detected in a diffraction pattern of the 2219SG alloy (Fig. 3b). The appearance of these peaks fits quite well with the presence of the Al_7Cu_2Fe phase.

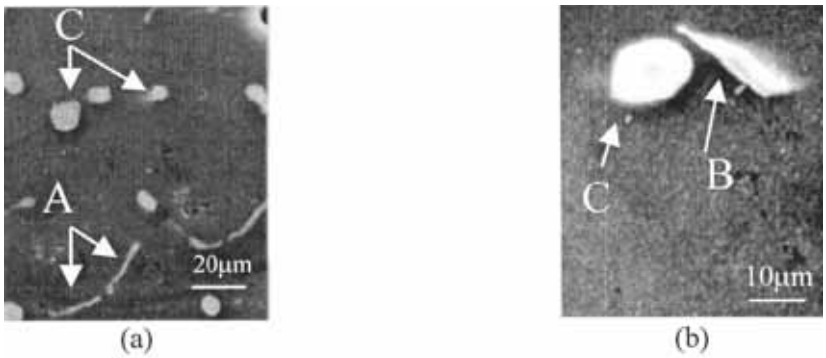

(a) (b)

Fig. 2. SEM micrographs. Microstrucrture of quenched samples. (a) Alloy 2219S; (b) alloy 2219SG. A – $(Fe, Mn, Cu)_3Si_2Al_{15}$ phase; B – Al_7Cu_2Fe phase; C – Al_2Cu phase.

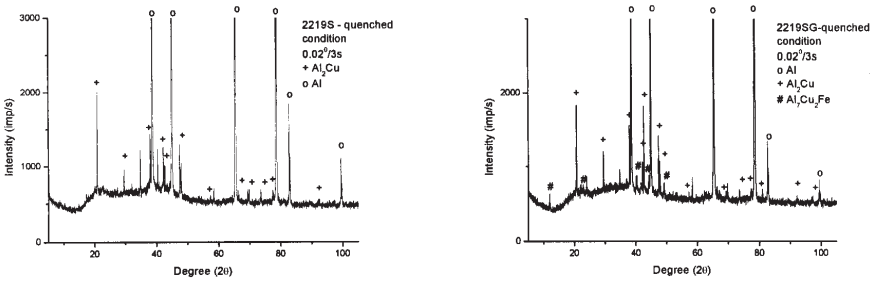

(a) (b)

Fig. 3. X-Ray diffraction of quenched samples. (a) Alloy 2219S; (b) alloy 2219SG.

TABLE II. Chemical analysis (EDS) of particles in quenched samples.

Alloy	Particle morphology	Element	mass %	at.%
2219S	Thin, long	Al	87.13	93.48
	(A)	Si	1.07	1.03
		Mn	2.40	1.19
		Fe	4.95	2.40
		Cu	4.46	1.90
	Globular	Al	71.65	87.89
	(C)	Cu	28.35	12.11
2219SG	Plate-like	O	0.95	1.59
	(B)	Al	73.04	86.88
		Mn	0.84	0.41
		Fe	5.56	2.75
		Cu	19.60	8.37
	Globular	Al	69.32	86.89
	(C)	Cu	30.68	13.11

Taking into account reflection of X-ray diffraction, it was found that a difference in the lattice parameters of the supersaturated solid solution of the two alloys exists, which indicates a different extent of supersaturation, especially considering Cu atoms. Lattice parameters of the Al-based supersaturated solid solution and the estimation of Cu concentration in this solid solution are given in Table III.

TABLE III. Lattice parameter of supersaturated Al solid solution and concentration of Cu solute atoms

Alloy	Lattice parameter a_{av} nm	*SE* x10^4	Concentration of Cu mass %
2219S	0.403887	7.8726	> 4.97
2219SG	0.404072	6.7123	≈ 4.3

**SE* – Standard error of the mean data

Concentration of Cu in the supersaturated solid solution was calculated using literature data for the binary Al–Cu system.[14] According to these data the amount of Cu (in mass %) varies from zero (for the lattice parameter $a = 0.40490$ nm) to 4.97 (for the lattice parameter $a = 0.40387$). The solubility of Cu in the solid solution of binary Al–based alloy at 500 ºC (which is the annealing temperature in this work) is about 4.4 mass %.[15] The results on concentration of Cu in the supersaturated solid solution should be regarded only as an approximate calculation, since the investigated materials are not binary Al–Cu alloys, but systems with rather complex chemical composition. Nevertheless, the enhanced concentration of Cu in the solid solution of 2219S alloy may be explained by the overall concentration of Si, considering that increased concentration of Si promotes the higher solubility of Cu in the Al-based solid solution.[16]

The results of X-ray diffraction and EDS analysis show that after quenching, besides the supersaturated solid solution (the matrix), some other phases are observed, *i.e.*:

$$\text{2219S alloy: water-quenching} \rightarrow \alpha_{S.S.S.} + Al_2Cu\ (\theta) + (Fe, Mn, Cu)_3Si_2Al_{15} \quad (1)$$

$$\text{2219SG alloy: water-quenching} \rightarrow \alpha_{S.S.S.} + Al_2Cu\ (\theta) + Al_7Cu_2Fe \quad (2)$$

where $\alpha_{S.S.S.}$ is the supersaturated solid solution of Al. (Fe, Mn, Cu)$_3$Si$_2$Al$_{15}$ and Al$_7$Cu$_2$Fe phases do not appear together in these alloys, the fact already established in some complex Al alloys.[13]

Change of hardness during aging. Change of hardness of 2219S and 2219SG alloys as a function of aging time at a constant temperature is shown in Fig. 4. Alloy 2219SG exhibits rapid hardening (up to 1 h) and a maximum at about 65 HRB is reached after 8 h of aging. During longer aging times hardness decreases approaching the level of about 50 HRB, which indicates that over-aging prevails as the operating process. Comparing to 2219SG, hardness of 2219S alloy slightly decreases at the beginning of aging which may be ascribed to reversion, *i.e.*, to the dissolution of GP zones formed during the previous process of artificial aging.[17] Maximum hardness at about 50 HRB (17 % less than the maximum of alloy 2219SG), is reached after 24 h, which is three times longer than for alloy 2219SG. After this maximum, the hardness of alloy 2219S significantly decreases with prolonged aging.

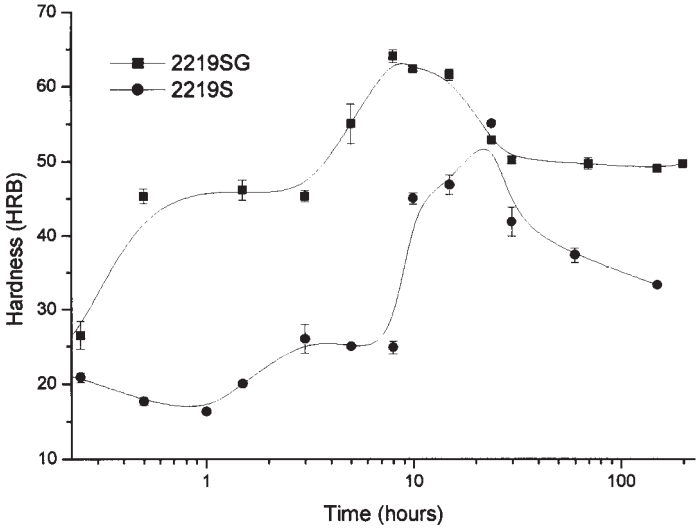

Fig. 4. Change of hardness during aging at 190 ºC.

Transmission electron microscopy. The microstructure of alloy 2219SG aged at the maximum hardness (after 8 h of aging) is shown in Fig. 5a,b. A selected area diffraction pattern (SADP) taken along the [001] matrix zone axis is characterized by weak streaks originating from coherent θ" particles (Fig. 5a). Edge-on θ" particles with diameters less than 100 nm are shown in Fig. 5b. The general sequence of the aging process of Al–Cu alloys is mostly described as: GP(1) zone → GP(2) zone or θ" → θ' → θ.[18] Maximum hardness on aging curves is associated with coherent precipitates, *i.e.*, θ" phase together with some θ' (the metastable form of the equilibrium θ phase, $CuAl_2$). In Al–4Cu–0.8Si–0.8Mg (mass %) alloy, the mixture of θ" and θ' phases at the maximum hardness was found at 130 ºC, whilst at 190 ºC only the θ' phase was associated with that maximum.[19] Weather the θ" and θ' mixture, or only

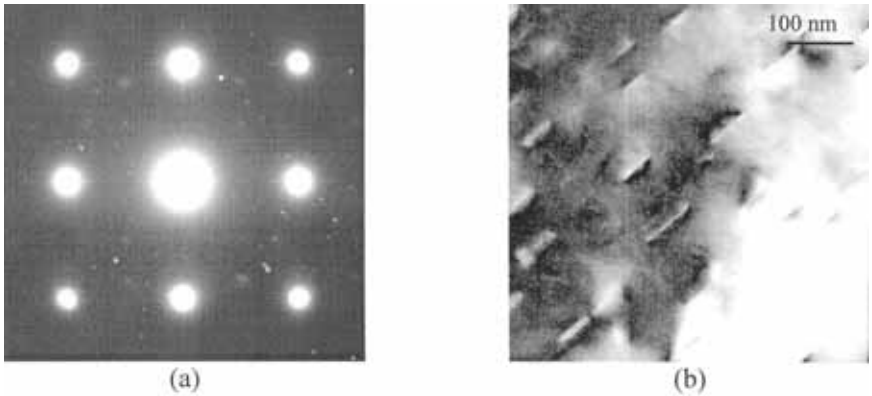

Fig. 5. TEM micrographs. Microstructure of alloy 2219SG aged at the maximum hardness (8 h at 190 ºC). (a) SADP along [001] matrix zone axis; (b) the bright field (BF) image showing θ" particles.

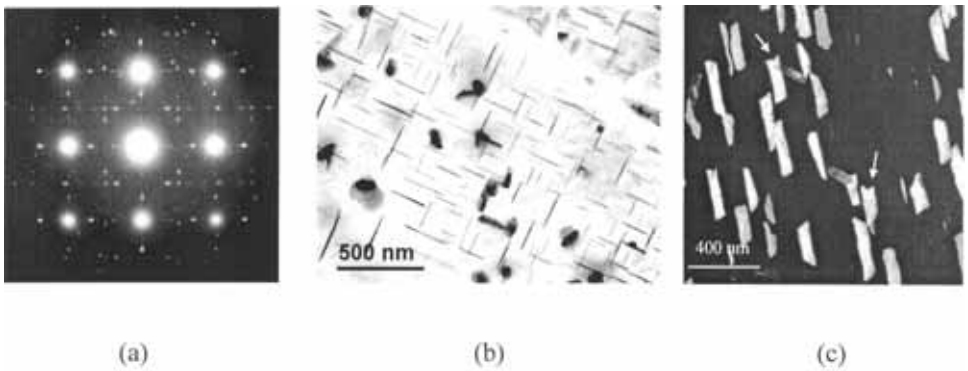

Fig. 6. TEM micrographs. Microstructure of over-aged alloy 2219SG (150 h at 190 ºC). (a) SADP along [001] matrix zone axis; (b) the bright field (BF) image showing θ' particles and rounded Si–Ge particles; (c) the dark-field (DF) image showing interaction of plate-like precipitates (θ') with Si–Ge particles (see arrows).

θ’ phase will be present at the hardness maximum depends on several parameters, such as concentration of copper, aging temperature and previous cold work. Microstructure after aging for 150 h is shown in Fig. 6a–c. SADP with additional spots corresponding to θ’ particles was taken along the [001] matrix zone axis (Fig. 6a). The bright-field image shows edge-on θ’ plates together with other equiaxed particles (Fig. 6b). The dark-field image which was obtained with the specimen tilted away from [011] matrix zone axis, shows that some θ’ phase precipitates interact with other precipitates, presumably Si–Ge particles (Fig. 6c). Since in an experimental alloy Al–0.5Si–0.5Ge (at.%) the appearance of Si–Ge particles was detected after 3 h of aging,[16] it is reasonable to suppose that these particles are also present in alloy 2219SG at the maximum hardness (although at a finer scale than after 150 h of aging) serving as nucleation sites for precipitation of θ” particles.

The microstructure of alloy 2219S after aging is shown in Fig. 7a,b for comparison. Figure 7a illustrates the bright-field image of the sample at the maximum hardness (after

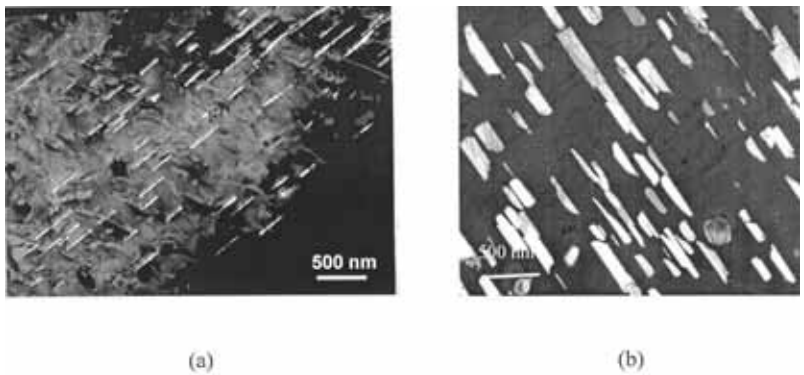

Fig. 7. TEM micrographs. DF image. Microstructure of alloy 2219S. (a) Aged at the maximum hardness (24 h at 190 ºC); (b) over-aged (150 h at 190 ºC).

24 h of aging) where thin edge-on θ' plates appear in the matrix, whereas Fig. 7b shows the dark-field image of θ' phase after aging for 150 h. It is clear that the limited over-aging after 150 h was controlled by the slow growth of θ' particles with diameters between 350 and 700 nm and thickness of about 100 nm.

Although there is some ambiguity on the issue whether not only θ'' phase, but a mixture of θ'' and θ' phases is present at the maximum hardness of alloy 2219SG, it is obvious that the addition of Ge in a commercial 2219 alloy promotes faster aging kinetics than in the alloy without Ge. Very fine Si–Ge precipitated particles were detected in the experimental quaternary Al–Cu–Si–Ge alloy aged at the maximum hardness (after 3 h).[16] Thus, it is reasonable to suppose that in the case of alloy 2219SG, Si–Ge particles are also present at th maximum hardness, although on much finer scale than after 150 h of aging. Accelerated aging kinetics in alloy 2219SG is a direct consequence of heterogeneous precipitation of Si–Ge particles representing energetically more favourable sites for precipitation of the θ'' phase. The significant effect of Ge addition on hardness is strongly confirmed by the fact that alloy 2219SG possesses higher hardness irrespective that the concentration of Cu, regarded as the most important hardening element, in this alloy is lower than in alloy 2219S (see Table III).

CONCLUSION

Applying microalloying, *i.e.*, by adding a very small amount of Ge to a commercial Al 2219 alloy and varying the concentration ratio of Si and Ge, changes of microstructure and hardness of two experimental alloys 2219S (without Ge) and 2219SG (with Ge) have been achieved.

After quenching, apart from the supersaturated solid solution, the equilibrium θ phase (Al_2Cu) is present in both alloys, as well as phases of the approximate chemical composition $(Fe, Mn, Cu)_3Si_2Al_{15}$ (2219S alloy) and Al_7Cu_2Fe (2219SG alloy).

Small addition of Ge promotes not only accelerated aging kinetics due to the presence of Si–Ge particles which serve as favourable sites for precipitation of fine coherent θ'' particles, but also increases the level of hardness compared to the alloy without Ge.

Acknowledgement: This investigation was a part of the project No. 1261 financed by The Ministry of Science, Technology and Development, Republic of Serbia. Authors are indebted to Miroslav Miljković from The University of Niš for provision of SEM facilities.

ИЗВОД

УТИЦАЈ МИКРОЛЕГИРАЊА СИЛИЦИЈУМОМ И ГЕРМАНИЈУМОМ НА МИКРОСТРУКТУРУ И ТВРДОЋУ КОМЕРЦИЈАЛНЕ ЛЕГУРЕ АЛУМИНИЈУМА

ВЕСНА МАКСИМОВИЋ[1], СЛАВИЦА ЗЕЦ[1], ВЕЛИМИР РАДМИЛОВИЋ[2] и МИЛАН Т. ЈОВАНОВИЋ[1]

[1]Лабораторија за материјале, Институт за нуклеарне науке "Винча", 11001 Београд, Србија и Црна Гора и [2]Department of Materials Science and Engineering, University of California, Berkeley, U.S.A.

Испитиван је утицај малих додатка Si и Ge на микроструктуру и тврдоћу за време старења комерцијалне легуре алуминијума 2219. Микролегирање утиче на микроструктуру легура и каљеном стању због различитог односа Si и Ge. Утврђено је да се при истом нивоу микролегирања максимум тврдоће у легури 2219SG (садржи Si и Ge) постиже три пута брже него у легури 2219S (без Ge). Убрзана кинетика таложења, последица је присуства Si–Ge талога који служе као места за хетерогено таложење θ" фазе која ојачава легуру.

(Примљено 1. априла, ревидирано 26. јуна 2003)

REFERENCES

1. S. P. Ringer, K. Hono, I. J. Polmear, T. Sakuraj, *Acta Metall.* **44** (1996) 1883
2. R. N. Wilson, *J. Inst. Metal.* **97** (1969) 80
3. J. Karov, W. V. Youdelis, *Mater. Sci. Technol.* **3** (1987) 1
4. J. M. Silcock, T. J. Heal, H. K. Hardy, *J. Inst. Metal.* **84** (1955) 23
5. J. D. Boyd, R. B. Nicholson, *Acta Metall.* **19** (1971) 1101
6. E. Hornbogen, A. K. Mukhopadahyay, E. A. Starke, Jr., *Z. Metallkd.* **83** (1992) 577
7. E. Hornbogen, A. K. Mukhopadahyay, E. A. Starke, Jr., *Script. Metall. Mater.* **27** (1992) 732
8. D. Mitlin, V. Radmilović, U. Dahmen, J. W. Morris, Jr., *Met. and Mat. Trans.* **32A** (2001) 197
9. V. Radmilović, U. Dahmen, J. W. Morris, will be submitted for Nature (2003)
10. V. Radmilović, U. Dahmen, B. Dracup, M. K. Miller, D. Mitlin, J. W. Morris, *Int. Conference on Aluminum Alloys*, Cambridge, 1–6 July (2002), UK
11. D. Mitlin, V. Radmilović, U. Dahmen, J. W. Morris, Jr., *Mater. Sci. Eng.* **A301** (2001) 232
12. J. E. Hatch, *Aluminum Properties and Physical Metallurgy*, (Russian translation) Moskva, Metallurgy, 1989, p. 215
13. L. F. Mondolfo, *Aluminum Alloys, Structure and Properties*, Butterworths, London, 1976, p. 208
14. W. P. Pearson, *A Handbook of Lattice Spacing and Structures of Metals and Alloys*, Pergamon Press, 1958, p. 328
15. H. Schuman, *Metalografija*, Beograd, TMF (1989) p. 531
16. D. Mitlin, *Ph. D. Thesis*, University of California, Berkeley, CA 94720 (2001)
17. D. A. Porter, K. E. Easterling, *Phase Transformations in Metals and Alloys*, Van Nostrad Reinhold (UK) Co. Ltd., 1983, pp. 291–308
18. J. W. Martin, *Precipitation Hardening*, Pergamon Press, Oxford, 1969, p. 142
19. W. Bonfield, *J. Mat. Sci.* **11** (1976) 1661.